Adv. Polar Upper Atmos. Res., **17**, 30–47, 2003

Lightning discharges in association with mesospheric optical phenomena in Japan and their effect on the lower ionosphere

Yasuhide Hobara[1], Masashi Hayakawa[2], Kenji Ohta[3] and Hiroshi Fukunishi[4]

[1] *LPCE/CNRS, Orleans, France*
[2] *Department of Electronic Engineering, The University of Electro-Communications, Chofu-shi, Tokyo 182-8585*
[3] *Department of Electronics Engineering, Chubu University, Kasugai, Aichi 487-8501*
[4] *Department of Astrophysics and Geophysics, Tohoku University, Sendai 980-8505*

(Received December 17, 2002; Accepted May 23, 2003)

Abstract: A quantitative and statistical analysis was performed using data from coordinated measurements consisting of ELF waves, VLF subionospheric disturbances and lightning discharges associated with transient luminous events (TLEs). These TLEs (sprites and elves) were observed during winter lightning storms over the Sea of Japan in the winter of 1998/99. A clear, straightforward relationship was found between the charge moment of the parent discharge, calculated from ELF ($f < 15$ Hz) transients, and the ionospheric disturbances, with a correlation coefficient of 0.97 independent of the type of TLEs; this suggests significant atmosphere-mesosphere-ionosphere coupling and implies that a large quasi-electrostatic (QE) field change occurring above lightning discharges with TLEs plays a significant role in modifying the electrical properties of the lower ionosphere. Sprites tend to be associated with large ionospheric disturbancs (-13~$+4.6$ dB, compared with the unperturbed waves) and a large charge moment (260–875 C·km), whereas a relatively large lightning peak current ($+223$~$+470$ kA,) (or a slow-tail amplitude) leading to a strong electromagnetic pulse (EMP) but with a rather small ionospheric disturbances seems to be necessary to initiate elves.

key words: mesospheric optical phenomena, lightning discharge, Trimpi effect, VLF propagation

1. Introduction

Recent observations of TLEs (transient luminous events) in the mesosphere at various places throughout the world have generated interest in the electrodynamic coupling of the lightning in the troposphere with that in the mesosphere and lower ionosphere. In Japan, TLEs were observed during winter thunderstorm activity over the Sea of Japan (Fukunishi *et al.*, 1999; Hayakawa *et al.*, 2002). Previous theories predict that sprites are produced by a large QE field as a result of the large positive charge that is lowered to the ground by during + cloud-to-ground (CG) discharges (Pasko *et al.*, 1995, 1997; Milikh *et al.*, 1995; Cho and Rycroft, 1998), while elves are believed to occur as a result of the direct heating of the lower ionosphere by the EMP produced by lightning (Nickolaenko and Hayakawa, 1995; Fukunishi *et al.*, 1996; Inan *et al.*, 1997).

Various electromagnetic phenomena associated with these optical events have been reported: (1) ELF transients (Nickolaenko and Hayakawa, 2002), (2) VLF scattering (Dowden *et al.*, 1996a, b, c; Inan *et al.*, 1996a, b, 1997) and (3) gamma-ray bursts (Boccippio *et al.*, 1995; Inan *et al.*, 1995, 1996a; Fishman *et al.*, 1994; Reising *et al.*, 1996). The characteristics of these various phenomena were summarized by Rodger (1999). To improve our understanding of the coupling mechanisms among tropospheric lightning, mesospheric optical phenomena, and the ionosphere, coordinated measurements are needed.

This paper is an extended and detailed version of our previous paper (Hobara *et al.*, 2001). In this paper, we present the results of our winter lightning campaign in which we observed phenomena associated with TLEs over the Japan Sea as a case study. To accomplish our objectives, we utilized optical measurements (consisting of CCD cameras and photometers installed by Tohoku University) to detect sprites and elves, ELF transient measurements to extract the charge moment of parent lightning strokes, and VLF scattering measurements as a sensitive tool for estimating ionospheric disturbances (electron temperature and density perturbations). The Japan Lightning Detection Network (JLDN), which covers all of Japan, allowed us to determine the location, onset time and peak current of the parent lightning discharges.

2. Observations

TLE data (onset time and the type of optical emission) for December 19, 1998, and January 22, 1999 were provided by Tohoku University, severe thunderstorms occurred in the Hokuriku area on these days. A low noise CCD camera and 16-channel array photometers were deployed to identify optical events. These instruments were installed at the Dodaira Astronomical Observatory (geographic coordinates: 36.0°N, 132°E) and at Sendai (38.3°N, 140.9°E). Elves were mainly identified by the accurate photometers, using the procedure described by Barrington-Leigh *et al.* (2001), while sprites were identified by the CCD camera. An ‘elves and sprite’ event was defined as a sprite that occurred within 0.2 ms of an elve onset.

Continuous wideband ELF transient measurements were performed at Moshiri, Hokkaido (geographic coordinates, 44.2°N, 142.2°E). We fully calibrated three field components (vertical electric field, Ez and two horizontal magnetic field components, Hew and Hns) in the frequency range of 1 to 800 Hz (with sampling frequency of 2 kHz). Notch filters were installed at the frequencies of 50 Hz, 100 Hz and 150 Hz for Ez, and at 50 Hz and 150 Hz for Hew and Hns. A GPS receiver provided an absolute time stamp for each sampling point. The arrival direction of the wave was determined using the simple goniometer method (Hayakawa, 1995); consisting of the following two steps: first, we estimated the arrival direction at each frequency (with 180° ambiguity); and second, by taking the phase difference between the E and H fields into account, we obtained the bearing angle lying on a particular quadrant after averaging it over a frequency range of 100 to 500 Hz. During this procedures, only frequency components satisfying the following two conditions were used to avoid significant errors in the estimated wave normal direction (bearing or azimuth): (1) the signal intensity (power spectrum of the transient signal) was at least 10 dB greater than that of the background, and (2) the phase difference between the two magnetic components was less than 40° to avoid large polarization errors (as suggested by Hayakawa, 1995). All the ELF events detected at Moshiri during the period of this study were found to have their wave normal directed towards the Hokuriku region, where the TLEs occurred.

Different VLF transmitter signals (NWC, NPM, NLK, NSS) were recorded continuously at Kasugai, Aichi (geographic coordinates: 35.25°N, 138.98°E), to monitor the ionospheric disturbances (Hayakawa, 2001a, b). This system (JAPAL) measures the amplitude and phase of the individual VLF transmitter signals using a highly accurate GPS timing unit with a time resolution of 100 ms.

The JLDN is based on a combined TOA (time of arrival)/MDF (magnetic direction finding) technology (Cummins *et al.*, 1998) that provides the absolute time, location and peak current of cloud to ground lightning discharges. We used these data to determine the location and peak current of the parent lightning discharges associated with the optical events.

The ELF field station (Moshiri) and the two sites where the TLE optical measurements were performed are shown in Fig. 1a. The distance between the region of thunderstorm activity and the ELF station (Moshiri) is about 1000 km. The location of the VLF receiving station (Kasugai) and the GCP (great circle path) of the VLF transmitter, North West Cape (NWC) (19.8 kHz) in Australia crossing the Kasugai station are shown in Fig. 1b (an enlarged view of the square area in Fig. 1a). Ionospheric perturbations near the GCP would significantly modify the amplitude and phase of the VLF signal detected at the Kasugai receiving station.

The onset times of events in each data set were compared with those of the optical events to identify events that were associated with optical events. In the case of the ELF data set, we selected events with an onset time of within ±100 ms from the onset of an optical event. Next, we performed a direction-finding analysis and selected the events coming from the Hokuriku region, based on their estimated bearings. As a result, all the ELF events detected at Moshiri in this study were found to have a wave normal directed toward the Hokuriku region, where the optical events occurred. Further, we excluded events that occurred prior to the parent lightning onset time, as obtained by the JLDN data. Considering the time resolution of our VLF scattering measurements, the following maehod was used to determine if an ionospheric perturbation had occurred in association with a particular optical event: (1) a 10-second frame (±5 s from the optical onset time) for the amplitude and phase variation of the VLF transmitter signal was selected and the mean value and standard deviation within the frame were caluculated; (2) the global maximum and minimum in amplitude and phase and its corresponding onset time were selected; (3) the peak magnitude should be above a value two times larger than the standard deviation and within ±1 s of the onset time of the optical event. We regard these signals as perturbations associated with sprites and/or elves. During our observation period, numerous TLEs were only detected on two days; the JLDN data for the Hokuriku area on these days was used in the analysis. Coincidences between the JLDN data and the optical events were determined based only on the time difference; events with a time difference of within ±100 ms from the TLE onset time were selected.

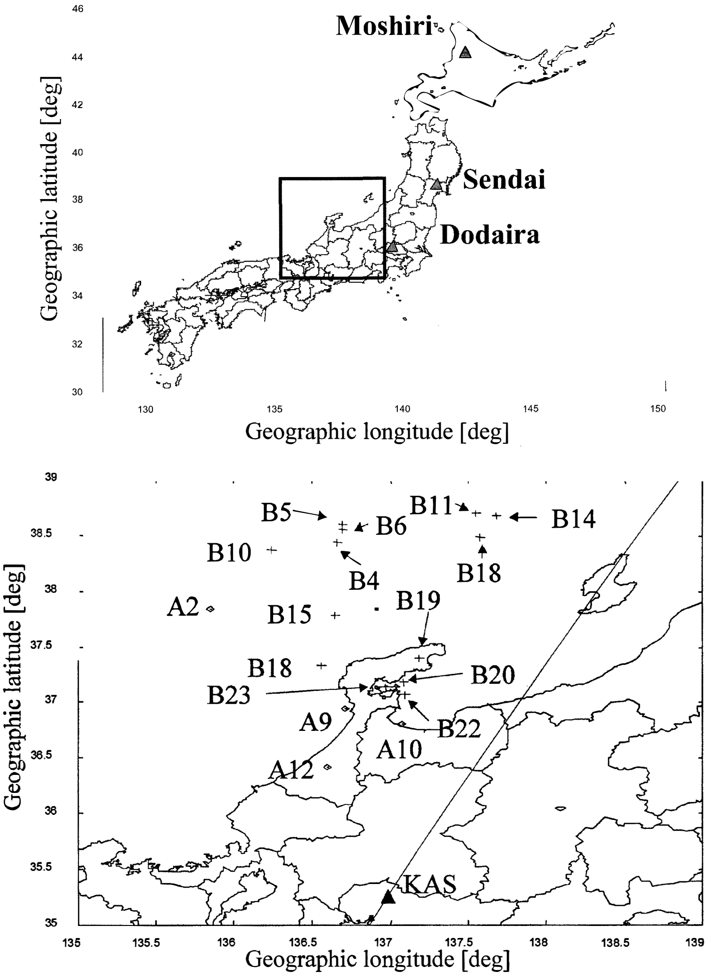

Fig. 1. (a) Locations of ELF field site (Moshiri) and optical measurements (Sendai and Dodaira) performed by Tohoku University. (b) Enlarged view of the square region in (a) showing the positions of the lightning discharges associated with TLEs, according to the JLDN data. The VLF (NWC) great circle path crossing Kasugai receiving station (KAS) is also shown.

3. TLEs on December 19, 1998

Here, we report the observations that were made on December 19, 1998, during the period of 1053–1825 UT, when optical emissions were observed during a severe winter thunderstorm over the Sea of Japan in the Hokuriku region.

During the period 0000–2000 UT, 477 CG discharges were detected by JLDN over the Hokuriku region, of which 47.6% (227 events) were positive strokes. The peak current of the lightning discharges ranged from −132 kA to +470 kA, with mean values for the positive and negative strokes of +81 kA, and −45 kA respectively. These characteristics of lightning discharges in winter are consistent with previous finding (*e.g.* Takeuti and Nakano, 1983). During the above-mentioned period, we detected 13 optical emissions; these emissions are summarized in Table 1. Eight events among them were identified as elves without any sprites, and the remaining events were only sprites or sprites with elves. According to the JLDN data, the parent lightning discharges of the optical events were located over the coastal region of the Noto-peninsula (A9, A10 and A12) and over the Japan Sea about ~100 km north-west of the peninsula (A2) (Fig. 1b). Despite the small number of events of each type of optical emission detected by the JLDN, elves- associated events seemed to have a large peak current of more than +400 kA, while events associated with carrot-type sprites had a peak current of only +39 kA. A similar tendency has been reported for continental summer lightning (*e.g.* Boccippio *et al.*, 1995). However, one exception occurred: event A12 seems to be a negative parent discharge with a rather small peak current of −30 kA. Barrington-Leigh and Inan (1999) reported that elves were only produced by −CGs. Here, we should comment on the reliability of the JLDN data. A recent study by Ishii *et al.* (2002) found that the detection rate for winter lightning in Japan by the JLDN was only about 70–80% of the value obtained using their own measurments, probably because the JLDN is a simple adoption of the American system that was developed for the detection of continental summer lightning (Cummins *et al.*, 1998). Thus, the JLDN system may not be extremely well suited for detecing Japanese winter lightning, since site errors and very complicated waveforms for winter lightning can be expected.

Figure 2 shows two typical time series of fully-calibrated ELF magnetic field waveforms for an event associated with an elves (A9) and a carrot-type sprite (A10); clear, transient signatures in the ELF range (Figs. 2a and 2b) can be seen and the corresponding amplitude spectra were calculated for 512 ms. One event associated with a sprite (A10) had a much smaller peak amplitude (~258 μA/m) than that of the other events associated with elves (A2, A9) (~731 μA/m, ~743 μA/m), as summarized in Table 1. The observed ELF peak amplitude ($f \leq 800$ Hz) was proportional to the peak current from the JLDN data. The polarity of the parent lightning was estimated

Table 1. Characteristics of parent lightning and VLF scattering properties for the event of December 19, 1998.

Event	Onsettime[UT] Hh:mm:ss.ms	Type	JLDN Peak Current[kA]	ELF Peak Amp. Peak Amp. [µA/m]	ELF Peak Amp. Polarity	Charge Moment Change Qds [C·km]	VLF(NWC) Scattering Amp.	VLF(NWC) Scattering Phs.	VLF(NWC) Amp.[dB]
A1	10:53:47.300	Elves							
A2	11:37:11.750	Elves	+409	731	+	150			
A3	13:45:50.200	Elves		506	+	122	*	*	-21.5
A4	13:52:24.410	Elves							
A5	16:12:45.460	D-Sprite		214	+	267	*	*	-4.1
A6	16:21:38.450	Sprite					*	*	-2.5
A7	16:26:03.560	Ca-Sprite					*	*	-12.3
A8	17:12:26.980	Elves					*	*	-3.5
A9	17:14:35.470	Elves	+470	743	+	175	*	*	-8.7
A10	17:38:52.890	Ca-Sprite	+39	258	+	301	*	*	+1.9
A11	17:43:11.280	Dn-Sprite	+111	337	+	338	*	*	+4.6
A12	18:12:45.200	Elves	-30						
A13	18:24:27.050	Elves		243	+	245			

D: Diet sprite Dn: Dancing sprite Ca: Carrot sprite E: Elves S:Sprite

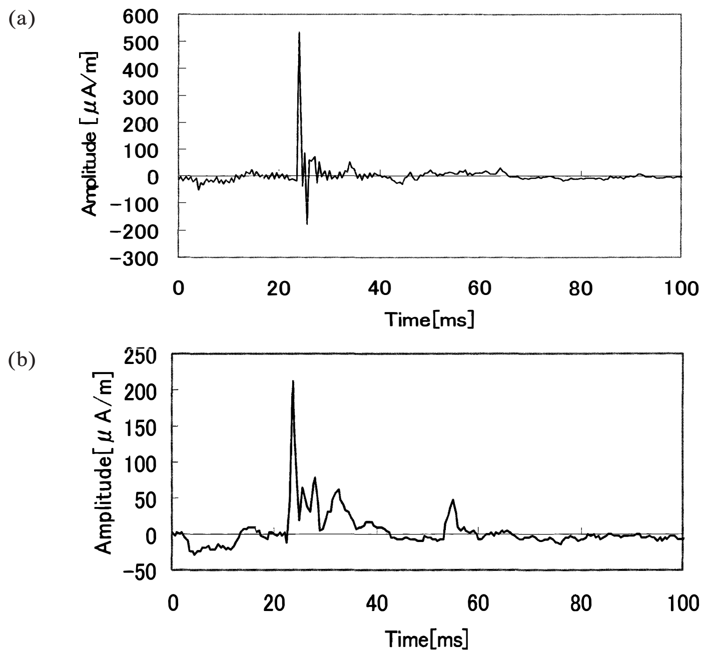

Fig. 2. (a) Time series for the waveform for the ELF magnetic field (Hew) associated with an elves (A9). (b) The same variation is seen for a carrot-type sprite (A10).

from the sign of the first excursion of Ez, and all the events had a positive polarity, coinciding with those from the JLDN peak current estimation (see Table 1).

The current moment of the ELF source in the frequency domain $I(f)$ was calculated from the amplitude spectrum of the magnetic field using normal mode equations (Wait, 1996; Jones, 1967; Ishaq and Jones, 1977; Nickolaenko and Hayakawa, 2002) with a small modification as shown below:

$$E_z = i\frac{I(f)ds\nu(\nu+1)P_\nu^0(-\cos\theta)}{4a^2\varepsilon_0 2\pi fh\sin(\pi\nu)}, \qquad [\mathrm{Vm}^{-1}\mathrm{Hz}^{-1}] \qquad (1)$$

$$H_\phi = -i\frac{I(f)dsP_\nu^1(-\cos\theta)}{4ah\sin(\pi\nu)}, \qquad [\mathrm{Am}^{-1}\mathrm{Hz}^{-1}] \qquad (2)$$

where $P_\nu^{0,1}$ are complex order Legendre functions; $\nu(f)$ is the dimensionless propagation constant at the wave frequency f; a and h are the Earth's radius (~6.4 Mm) and the effective height of the ionosphere, respectively; ε_0 is the dielectric constant of free space; and θ is the great circle distance between the source and the receiver. Furthermore, $I(f)ds$ is the current moment of the source, where $I(f)$ is the current in amperes and ds is the vertical distance that this current flows. Using the amplitude spectra obtained from the observations and eqs. (1) and (2), the current moment can be calculated.

In this study, we used a source-observer distance of 1 Mm, which is a reasonable value between Moshiri and the location of the events in the Hokuriku area; the results for $I(f)ds$ were derived using the magnetic field component, since Ez has a relatively large interference, compared to that of the H fields.

The frequency dependencies of the calculated current moment for the different ELF events are shown in Fig. 3a. For sprite-producing discharges (A5, A10 and A11), the current moments were estimated to be large (the three largest current moments among all the events) for the lower frequency range ($f \leq 50$ Hz) and small for the high frequency range (50 Hz $\leq f \leq$ 1000 Hz). While elves-producing discharges (A3 and A9) exhibit smaller current moments ($f \leq 50$ Hz) than sprite events, they also exhibit a higher frequency component ($f \geq 100$ Hz), which contributes to the ELF slow-tail and is the main contributor to the ELF peak amplitude in the time series. The frequency characteristics described above are similar to the previously reported results of Huang *et al.* (1999), with a white-noise-like spectrum for elves and a red-noise-like spectrum for sprites.

Based on the frequency spectrum of the source current moment, we attempted to estimate the charge moment using impulsive approximation (Huang *et al.*, 1999). In this method, we assumed the lightning current to have an exponential form in the time

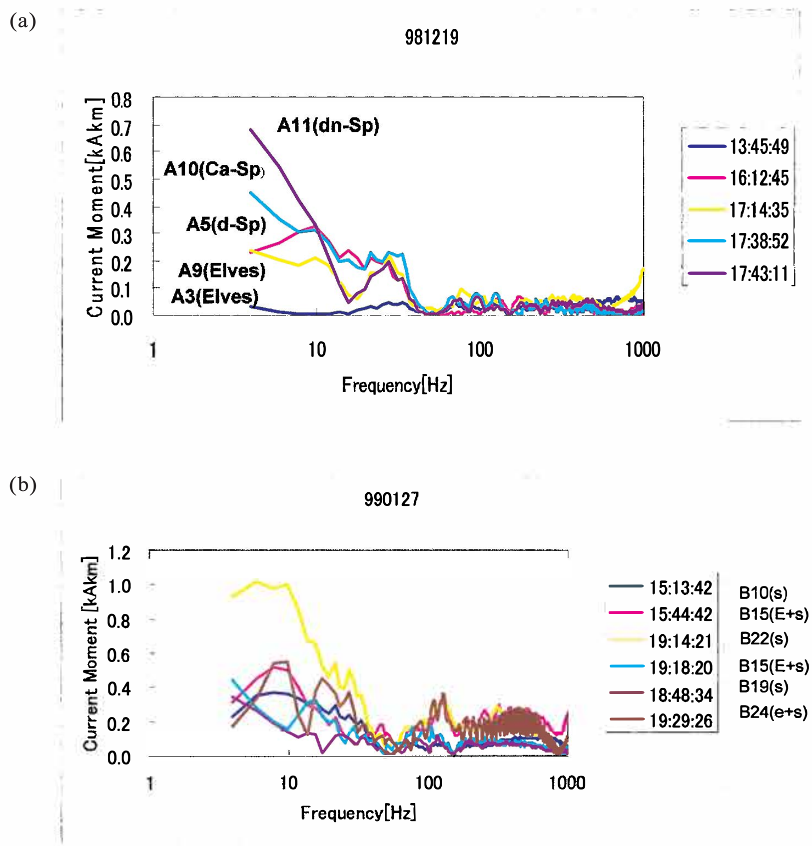

Fig. 3. (a) Current moments calculated from the ELF transients (magnetic field) for the different optical events that occurred on December 19, 1998. (b) A similar tendency is seen for the events that occurred on January 27, 1999.

domain ($I(t) = I_0 e^{-t/\tau}$). With the $\tau \to 0$ limitation in its frequency domain $I(f)$ can be replaced with Qds after a Fourier transformation. Despite the underestimation of Qds for any event with a finite time constant τ, this estimation can provide quantitative information on the charge transfer between the events. The averaged Qds were derived using the frequency range ($f \leq 15$ Hz). Sprite-producing discharges had a larger charge moment, with a mean value of 302 C·km, than those for elves-producing discharges (mean value, 150 C·km), as summarized in Table 1. This mean value for sprites is in the range of the corresponding values deduced from ELF transients in the U.S. (Huang *et al.*, 1999; Bell *et al.*, 1998; Cummer and Inan, 1997; Cummer and Stanley, 1999; Hu *et al.*, 2002).

Figure 4a illustrates the VLF experiment used to derive the ionospheric disturbances. The electric field of the VLF transmitter signal from NWC (Australia) (indicated by VLF TMR) is continuously monitored at Kasugai (VLF RCVR). When an ionospheric perturbation occurs as a result of an external effect (here we expect EMP heating, QE heating and possibly the sprite itself) on the GCP crossing the transmitter and receiver, particularly within the first Fresnel zone, a sudden change in the amplitude and phase variation of the receiving signals is observed.

Figure 5 shows two examples of well-defined VLF perturbations associated with an elves (A9) and a sprite (A11) that exhibited an early/fast or a RORD (Rapid Onset Rapid Decay) Trimpi (Dowden *et al.*, 1996a; Inan *et al.*, 1996b). Both the amplitude and the phase have bipolar structures (negative peak followed by a positive increase over time). However, only one peak is well above a value that is two times larger than the standard deviation (σ) in the amplitude or phase calculated within the frame for each case.

Figure 4b illustrates the relationship between the field vectors before and after the onset of a VLF Trimpi. Before the onset of the VLF event, the direct field vector from the transmitter is seen as an unperturbed field vector (mean value in the frame here) and the total field vector is observed after the onset and corresponds to a vector addition of the direct and scattered field vectors. So, the scattered field vector is easily derived by phasor subtraction. As a result, the scattered field vector is calculated in terms of the

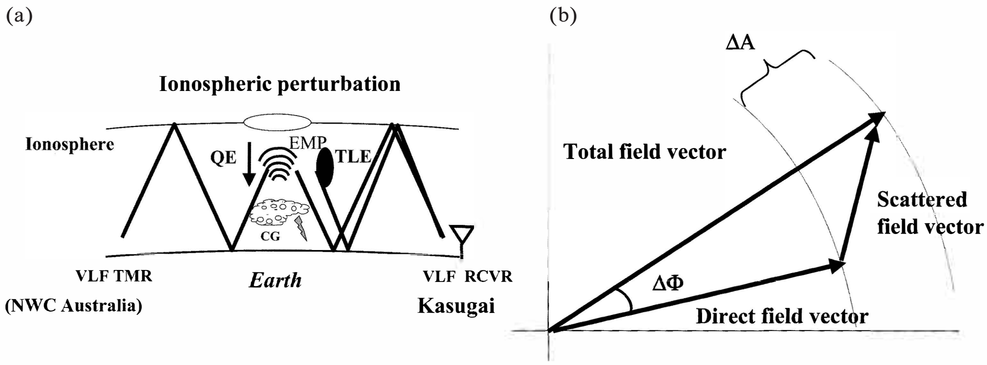

Fig. 4. (a) Schematic picture of the VLF monitoring system used to detect ionospheric perturbations. (b) The phasor concept was used to derive the scattered signal. The direct field represents the unpertured signal.

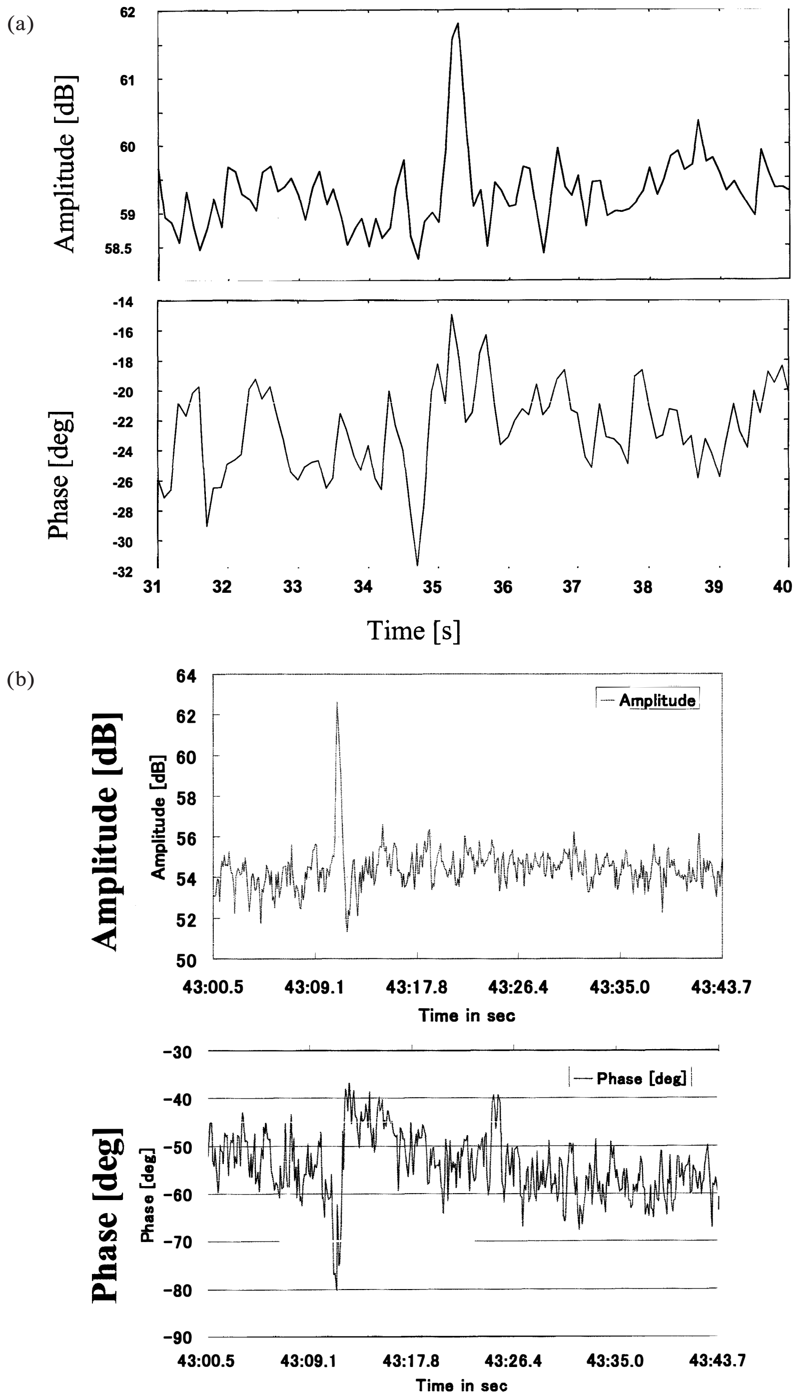

Fig. 5. (a) The NWC-KAS VLF signal amplitude for an elve (A9) is shown in the top panel, whereas the corresponding phase is shown in the bottom panel. (b) The same parameters as in (a), but for a sprite (A11).

magnitude and phase of the scattered signal with reference to the unperturbed signal, indicating the magnitude of the ionospheric perturbation.

We derived the amplitudes of the scattered signals as −8.67 dB and +4.6 dB for A9 and A11, respectively. Performing similar analyses for the remaining VLF events, we obtained a scattered field ranging from −21.49 dB to +4.60 dB for 8 events (see Table 1). Among these events, the mean scattered amplitude of the elves (A3, A8 and A9) was −11.22 dB, which is significantly smaller than the −2.49 dB of sprites (A5, A6, A7, A10 and A11). Two post-onset type events (Inan *et al.*, 1996b) were found (A10 and A11) in association with sprites. Only two causative discharges were identified by the JLDN (A9 and A10); these discharges were located on the east and west side of the south-central region of the Noto-peninsula, ~150 km west of the NWC-Kasugai GCP and ~200 km northwest of Kasugai station. The absence of causative lightning discharges in the JLDN data may have something to do with the system performance of the network, as mentioned ealier (Ishii *et al.*, 2002). Considering the lightning activity from all JLDN onset locations, the remaining events would have also occurred over the Japan Sea and the coastal region of the Noto-peninsula in the Hokuriku region. This may suggest that all the VLF events were caused by the rather strong scattered signals from the source region, despite the fact that most sources of the VLF perturbations were located withn ±50 km of the GCP (Inan *et al.*, 1995).

4. TLEs on January 27, 1999

Table 2 shows a summary of the optical events and associated JLDN lightning events, ELF transients and VLF scattering measurements performed during the period of 1322–1930 UT on January 27, 1999. Nine elves without sprites and sixteen sprites or sprites with elves were detected optically.

The JLDN identified 13 parent discharges associated with the optical events, with peak currents ranging from +44 kA to +371 kA. The total flash number during this observation period was smaller than that on December 19 (411 events), but the mean peak current for the positive discharges, accounting for 44.5% of the total events, had a larger value (~+96 kA). Furthermore, the peak currents of the parent lightning for the elves were relatively large (+232 kA for B6 and +371 kA for B18), compared with those for the sprite-producing lightning discharges shown in Table 2. The location of these CGs is shown in Fig. 1b.

The peak amplitudes of the ELF transients for several sprite-producing lightning discharges were larger than 1000 μA/m, whereas elves events without a sprite were associated with smaller peak current values (<600 μA/m), similar to the results obtained for the December events. For example, the peak amplitude of B22, a sprite-associated event, was +231 kA; this value is larger than that of the A9 event occuring in December, event A9 in spite of a much larger peak current (+470 kA). These observations suggest that the source characteristics in the ELF range have a much large effect on the amplitude difference on these two days than the propagation effect, since the spatial separation of these two events was only about 50 km. As for the polarity determined by the Ez component, all the events expect one (B13) appeared to have a positive polarity; since no JLDN data for the B13 event was available, its polarity could

Table 2. Characteristics of parent lightning and VLF scattering properties for the event of January 27, 1999.

Event	Onsettime[UT] Hh:mm:ss.ms	Type	JLDN Peak Current[kA]	ELF Peak Amp. Peak Amp. [μA/m]	ELF Peak Amp. Polarity	Charge Moment Change Qds [C·km]	VLF(NWC) Amp.	VLF(NWC) Phs.	VLF(NWC) Scattering Amp.[dB]
B1	13:22:45.000	Elves							
B2	13:24:54.000	Elves							
B3	13:52:05.000	Elves							
B4	14:24:22.690	Sprite(FOV)	+120				*	*	-8.4
B5	14:33:18.830	Sprite(FOV)	+135				*	*	-11.7
B6	14:37:10.440	Elves?	+232				*	*	-13.8
B7	14:46:06.000	Elves					*	*	-17.9
B8	14:47:41.280	cf+Elves		599	+	121		*	
B9	14:50:27.970	cf+E,E+S					*	*	-17.0
B10	15:13:42.900	Sprite(FOV)	+141	919	+	324	*	*	-15.7
B11	15:19:01.100	Sprite	+78				*	*	-12.0
B12	15:26:10.670	Sprite	+130	1029	+	260	-	-	
B13	15:29:13.660	Elves+Sprite		1338	-	585	*	*	-18.6
B14	15:30:21.580	Sprite	+138				*	*	-13.8
B15	15:44:42.940	Elves+Sprite(FOV)	+223	1641	+	394	*	*	-14.8
B16	15:47:04.000	cf+Elves		1385		(202)	*	*	-12.5
B17	16:36:51.660	cf+Elves		580	+	847	-	-	
B18	17:52:22.340	cf+Elves?	+371				*	*	-7.7
B19	18:48:34.380	Sprite	+48	478	+		-	*	
B20	19:01:15.420	Sprite	+44				-	-	
B21	19:09:13.440	Sprite		279			*	*	-4.3
B22	19:14:21.540	Sprite	+231	1289	+	876	*	*	-13.2
B23	19:18:20.660	Sprite	+81	632	+	280	*	*	-12.8
B24	19:29:26.950	Elves+Sprite							
B25	19:29:26.840	Elves+Sprite		1267	+	335	*	*	-9.0

FOV: Field of view cf: Cloud flash

not be determined.

The most significant difference in the ELF data for the two different observation days was the estimated current moment. The frequency dependence of the current moment for a sprite-producing discharge (B22) had a red noise-like spectrum ($f<100$ Hz). However, another enhancement in the slow-tail frequency range ($100\,\text{Hz}<f<1000\,\text{Hz}$), which did not exist in the December event (Fig. 3b) could be clearly identified even after taking into account the effect of the notch filters installed at 50 Hz and 150 Hz, leading to a large peak amplitude. In contrast, an elves-producing discharge (without a sprite) (B8) was found to have a similar frequency dependence (white noise-like spectrum) and nearly the same Ids values as the December events.

The Qds calculated using the same method as described for the December case ranged from 121 to 876 C·km. The B17 event exhibited a different nature from that of the other elves-producing discharges in that it possessed quite a large charge moment of ~847 C·km, the second largest value of all the events. Probably this transient was not an elves-associated events since this is the only case where the onset was prior to the optical event (−2 ms). In Janurary, only one elves-producing event (B8) exhibited a smaller Q on the order of the December event. The mean charge moment for the sprite-producing and sprite-with-elves-producing events was 488 C·km, which was larger than that for the December events.

Scattered VLF fields calculated from the amplitude and phase change before and after the corresponding optical event were within a smaller range, from −18.64 dB to

−4.34 dB, compared with that of the December case. Little difference was seen in the magnitude of the sprite- and elves-associated events, whose mean values were −12.61 dB and −12.96 dB, respectively; this result contrasts that for the December events, for which a distinct different was seen. No clear explanation for the difference in the detectability of each event has been bade, but this matter may be strongly related to lower ionospheric conditions that affect the propagation of the VLF transmitter signals.

5. Comparison of the experiments

Figures 6 and 7 summarize the parameters of the different types of TLEs observed on December 19 and January 27, respectively. A box in the panel indicates the value of each event for the four parameters (Ip, ELF peak amplitude, Qds and VLF scattering amplitude, from top to bottom). The two right-most bars are the mean values of each separate parameter for an elves (indicated by E) and a sprite (S). As is seen from the figures, not all the events produced the different parameters simultaneously. As far as the mean value is concerned, however, the peak current (Ip) and the ELF peak amplitude exhibited similar tendencies, with a large mean value for elves and a small mean value for sprites. This result, together with the previous results, may imply that a large EMP is necessary for the generation of elves. On the contrary, the charge moment (Qds) and VLF scattered amplitude were found to have opposite characteristics; that is, large values for sprites and small values for elves. In other words, a sprite requires a large QE field and produces a large ionospheric perturbation. In the case of the January event shown in Fig. 7, all of the paramenters showed similar tendencies to those seen for the December events except for the ionospheric perturbation. The scattered signal intensity between the sprite and elves cases was nearly the same in Fig. 7, which probably indicates that the response of the ionosphere was quite different on the two days shown in Figs. 6 and 7.

The JLDN peak current is plotted as a function of the ELF peak amplitude in Fig. 8a. The peak amplitude was well correlated with the peak current for the sprite-producing discharges in both December and January. A correlation coefficient of $r=0.98$ was obtained for the December events (indicated by the circles), and a value of $r=0.95$ was obtained for the January events (indicated by the triangles). However, the slope for the December event was significantly larger than that for the January event; this difference may be attributed to the existence of energy in the slow-tail frequency band. Nevertheless, these large correlation coefficients are understandable because the JLDN uses the VLF frequency range to estimate the peak current.

Figure 8b shows the relationship between the estimated charge moment and the ELF peak amplitude. For the December events, two clusters can be clearly identified in the distribution. The first group has a large ELF peak amplitude and a small charge moment Qds, so the EMP is intensively generated, rather than a QE field change, leading to the generation of elves. The other group has a large charge moment with a small ELF amplitude, so a considerably large QE field change is expected, as opposed to an EMP. This group seemed to preferentially generate sprites with the exception of an A 13 (elve). However, the estimated charge moment value increased as the ELF peak amplitude increased as far as the same type of optical event is concerned. The January

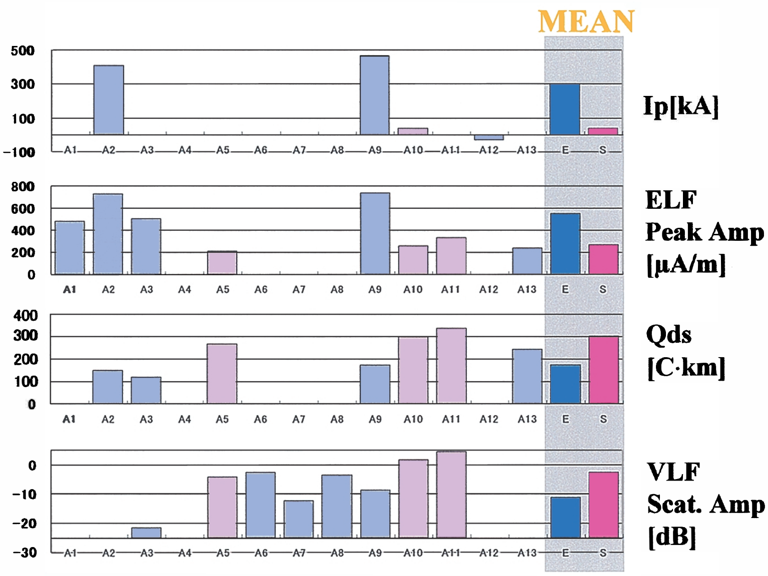

Fig. 6. Summary of the different parameters for different types of TLEs observed on December 19.

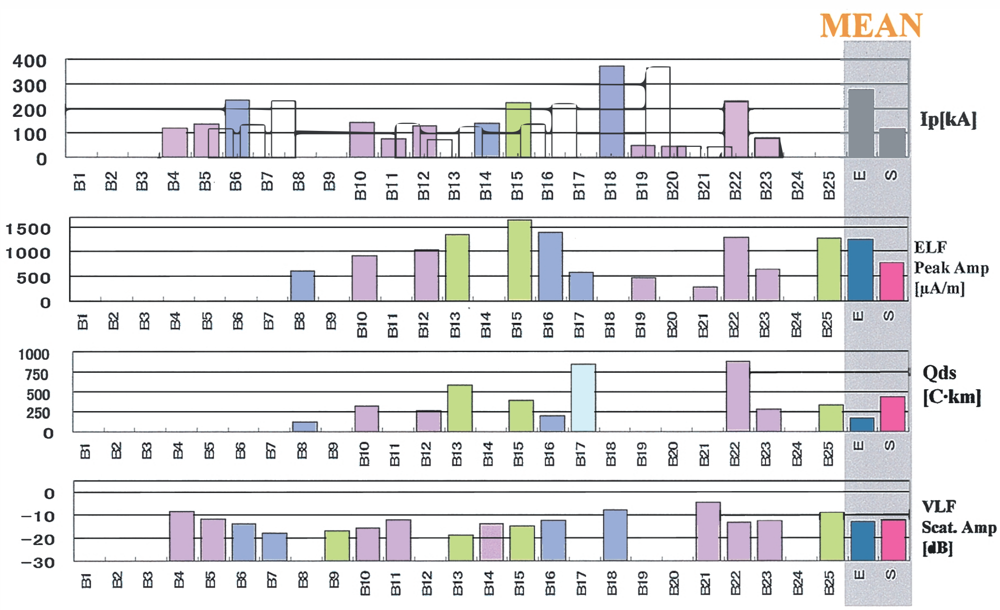

Fig. 7. Summary of the different parameters for different types of TLEs observed on January 27.

events exhibited a nearly random distribution and had a weak correlation coefficient ($r=0.07$), but either the ELF amplitude or the Qds was much greater than those for the December events. Moreover, all the events seemed to exceed the threshold values, depending on the type of TLEs. Accordingly, elves seem to occur when a rather large

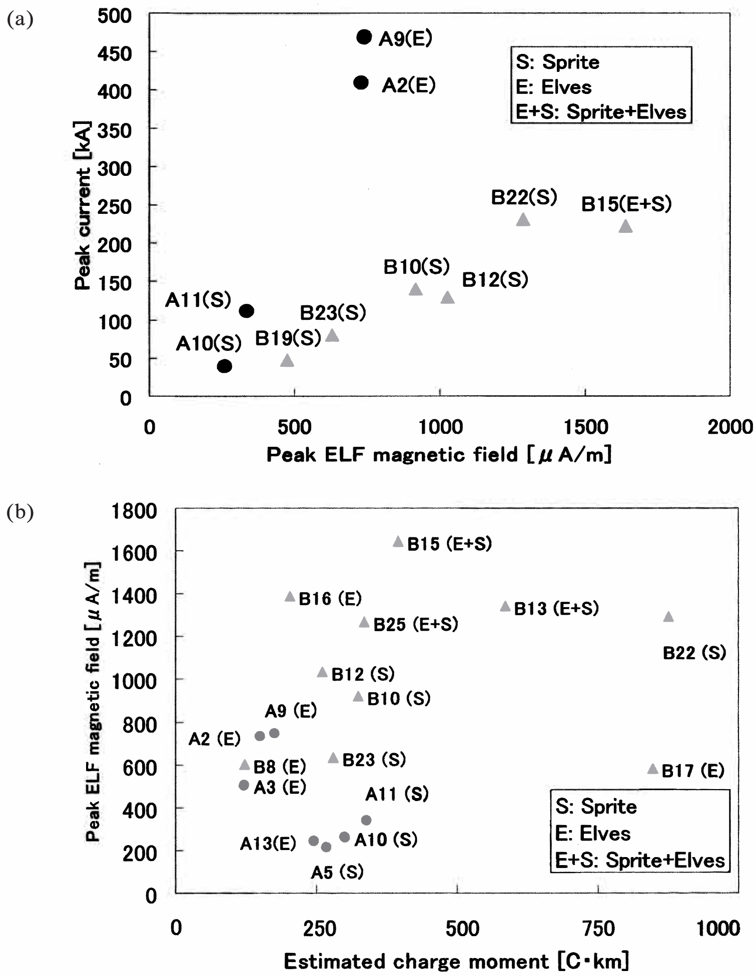

Fig. 8. *(a) JLDN peak current as a function of ELF peak amplitude on two different days. (b) ELF peak amplitude as a function of the estimated charge moment.*

peak amplitude (>100 μA/m) is present, while sprites are generated by quite a large charge transfer (>325 C・km).

The magnitude of the ionospheric perturbations as a function of the ELF amplitude is shown in Fig. 8c. As seen from the figure, the peak ELF amplitude was not a primary factor in controlling the scattered amplitude. One of the most striking features seen in this study was the clear, straightforward relationship between the charge moment and the VLF scattered field for the December 19 events, which had quite a high correlation coefficient of r=0.97 (Fig. 8d). Sprite-producing discharges (A10, A11 and A5) with a large charge moment had a large scattered field; in particular, a dancing sprite (A11) had the largest charge moment and scattered field among these discharges. The elves-producing events (A3 and A9), on the other hand, had a small charge moment and a small scattered field. Moreover, the peak current (or ELF peak amplitude) was

(c)

(d)

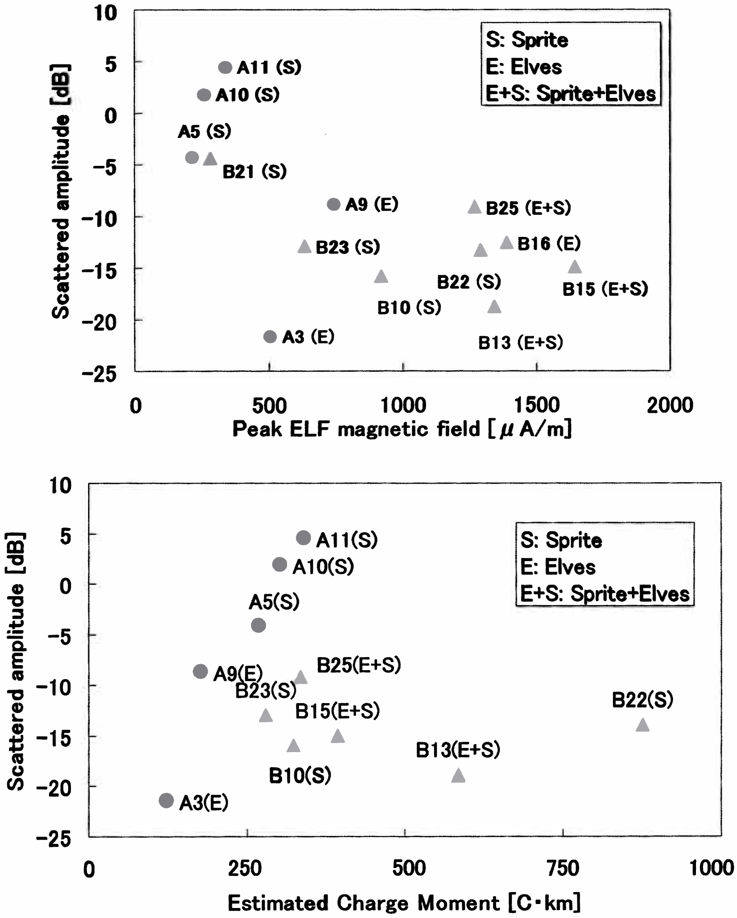

Fig. 8. (c) VLF scattered field (NWC) received at KAS as a function of the ELF peak amplitude. (d) VLF scattered field (NWC) received at KAS as a function of the charge moment, calculated from ELF transients.

not clearly related to the VLF scattered field, as seen in Fig. 8c and in a recent work by Johnson *et al.* (1999). For the January event, only sprite-associated scattered field were detected, and all the events had rather large charge moments that would have been sufficient to excite sprites; however, all the scattered fields were quite small, and no clear relationship was seen between the charge moment and the scattered amplitude ($r = 0.28$). The quantitative discrepancy in the scattered amplitudes for the two days may be due to the differences in the ambient conductivity of the *D*-region produced by QE thundercloud fields during the storm activity. According to the JLDN data, the storm region on December 19 was much closer to land than the storm region on January 27, and this difference may have strongly influenced the lower ionosphere around the scattered path between the source and Kasugai station.

To summarized this section, the magnitude of the QE-localized heating over the lightning discharges associated with optical events as a result of a large positive charge movement to the ground, characterized by Qds, determined the scattered field magnitude attributed to the modification of the *D*-region. While EMP heating in association with elves seems to be less effective at changing the conductivity in the ionosphere, we have not yet determined how the sprite-associated ionization columns in the mesosphere (Dowden *et al.*, 1996a, b, c) effectively reflect the VLF signals or we have to study whether the idea of such ionization columns would really work or not, compared with the above-mentioned local QE heating case.

6. Conclusion

We statistically analyzed the results of a coordinated campaign performed during periods of winter lightning activity over the Japan Sea; these results included measurements of mesospheric optical emissions, ELF transients, subionospheric VLF signal perturbations and lightning detection network data. On the two days when optical events were detected by Fukunishi *et al.* (1999), we have found several important feature suggestive of atmosphere-mesosphere-ionosphere coupling. These features are summarized below:

(1) The magnitude of the ionospheric disturbances in associated with mesospheric TLEs was positively correlated with the charge moment, deduced from the averaged current moment of the low frequency component of ELF transients ($f<15$ Hz) (correlation coefficient $r=0.97$ for December events); however, this relationship was sensitive to the ionospheric conditions.

(2) A positive correlation between the slow-tail component in the ELF range (frequencies of a few hundred Hz) and the peak current, based on the JLDN data (observed at a much higher frequency), was found ($r\geq0.95$), but neither of these parameters were the major determinant of the magnitude of ionospheric perturbations.

(3) Sprites tended to occur in association with parent lightning discharge that had a relatively large positive charge moment during our observation period (Qds$>$250 C·km), even if they possessed a small peak current for the slow-tail amplitude, whereas elves may have a much smaller charge moment threshold but require a sufficiently large peak current (or slow-tail amplitude). (4) By combining the above results (1) and (3), QE heating in relation to sprites and/or ionized columns produced by sprites may be the most important parameter affecting the magnitude of ionospheric perturbations, rather than EMP heating from elves-producing discharges and/or elves themselves.

Acknowledgements

The authors thank the anonymous referees for their constructive comments in reviewing the paper. This work was partly supported by National Institute of Polar Research (Tokyo), to which we are grateful.

The editor thanks Dr. Z. Kawasaki and another referee for their help in evaluating this paper.

References

Barrington-Leigh, C.P. and Inan, U.S. (1999): Elves triggered by positive and negative lightning discharges. Geophys. Res. Lett., **26**, 683–686.

Barrington-Leigh, C.P., Inan U.S. and Stanley, M. (2001): Identification of sprites and elves with intensified video and broadband array photometry. J. Geophys. Res., **106**, 1741–1750.

Bell, T.F., Reising, S.C. and Inan, U.S. (1998): Intense continuing currents following positive cloud-to-ground lightning associated with red sprites. Geophys. Res. Lett., **25**, 1285–1288.

Boccippio, D.J., Williams, E.R., Heckman, S.J., Lyons, W.A., Baker, I.T. and Boldi, R. (1995): Sprites, ELF transients and positive ground strokes. Science, **269**, 1088–1091.

Cho, M. and Rycroft, M.J. (1998): Computer simulation of the electric field structure and optical emissions from cloud-top to the ionosphere. J. Atmos. Solar-Terr. Phys., **60**, 871–888.

Cummer, S.A. and Inan, U.S. (1997): Measurement of charge transfer in sprite-producing lightning using ELF radio atmospherics. Geophys. Res. Lett., **24**, 1731–1734.

Cummer, S.A. and Stanley, M. (1999): Submillisecond resolution lightning currents and sprite development: observations and implications. Geophys. Res. Lett., **26**, 3205–3208.

Cummins, K.L., Murphy, M.J., Bardo, E.A., Hiscox, N.L., Pyle, R.B. and Pifer, A.E. (1998): A combined TOA/MDF technology upgrade of the U. S. National Lightning Detection Network. J. Geophys. Res., **103**, 9035–9044.

Dowden, R.L., Brundell, J.B. and Lyons, W.A. (1996a): Are VLF rapid onset, rapid decay perturbations produced by scattering off sprite plasma? J. Geophys. Res., **101**, 19175–19184.

Dowden, R.L., Brundell, J.B., Lyons, W.A. and Nelson, T. (1996b): Detection and location of red sprites by VLF scattering of subionospheric transmitters. Geophys. Res. Lett., **23**, 1737–1740.

Dowden, R.L., Brundell, J.B., Rodger, C.J., Molchanov, O.A., Lyons, W. and Nelson, T. (1996c): The structure of red sprites determined by VLF scattering. IEEE Antennas Propag. Mag., **38** (3), 7–15.

Fishman, G.J., Bhat, P.N., Mallozzi, R., Horack, J.M., Koshut, T., Kouveliotou, C., Pendleton, G.N., Meegan, C.A., Wilson, R.B., Paciesas, W.S., Goodman, S.J. and Christian, H.J. (1994): Discovery of intense gamma-ray flashes of atmospheric origin. Science, **264**, 1313–1316.

Fukunishi, H., Takahashi, Y., Kubota, M., Sakanoi, K., Inan, U.S. and Lyons, W.A. (1996): Elves: Lightning-induced transient luminous events in the lower ionosphere. Geophys. Res. Lett., **23**, 2157–2160.

Fukunishi, H., Takahashi, Y., Uchida, A., Sera, M., Adachi, K. and Miyasato, R. (1999): Occurrences of sprites and elves above the Sea of Japan near Hokuriku in winter. EOS, **80** (46), F217.

Hayakawa, M. (1995): Whistlers. Handbook of Atmospheric Electrodynamics, Vol. 2, ed. by H. Volland. CRC Press, 155–193.

Hayakawa, M. (2001a): NASDA's Earthquake Remote Sensing Frontier Research, Electromagnetic Phenomena in the Lithosphere, Atmosphere and Ionosphere, Final Report. Univ. of Electro-Communications, 288 p.

Hayakawa, M. (2001b): Electromagnetic phenomena associated with earthquakes: Reviews. Trans. Inst. Electr. Engrs. Jpn., **121-A**, 893–898.

Hayakawa, M., Nakamura, T., Hobara, Y. and Otsuyama, T. (2002): Mesospheric optical events in association with lightning discharge and related phenomena. Oyo Kogaku (Appl. Optics), **1**, 14–21 (in Japanese).

Hobara, Y., Iwasaki, N., Hayashida, T., Hayakawa, M., Ohta, K. and Fukunishi, H. (2001): Interrelation between ELF transients and ionospheric disturbances in association with sprites and elves. Geophys. Res. Lett., **28**, 935–938.

Hu, W.Y., Cummer, S.A. and Lyons, W.A. (2002): Lightning charge moment changes for the initiation of sprites. Geophys. Res. Lett., **29**, doi: 10.1029/2001 GL 014593.

Huang, E., Williams, E., Boldi, R., Heckman, S., Lyons, W., Taylor, M., Nelson, T. and Wong, C. (1999): Criteria for sprites and elves based on Schumann resonance observations. J. Geophys. Res., **104**, 16943–16964.

Inan, U.S., Bell, T.F., Pasko, V.P., Sentman, D.D., Wescott, E.M. and Lyons, W.A. (1995): VLF signatures of ionospheric disturbances associated with sprites. Geophys. Res. Lett., **22**, 3461–3464.

Inan, U.S., Reising, S.C., Fishman, G.J. and Horack, J.M. (1996a): On the association of terrestrial gamma-ray bursts with lightning and implications for sprites. Geophys. Res. Lett., **23**, 1017–1020.

Inan, U.S., Slingeland, A. and Pasko, V.P. (1996b): VLF and LF signatures of mesospheric/lower ionospheric response to lightning discharges. J. Geophys. Res., **101**, 5219–5238.

Inan, U.S., Barrington-Leigh, C., Hansen, S., Glukhov, V.S., Bell, T.F. and Rairden, R. (1997): Rapid lateral expansion of optical luminosity in lightning-induced ionospheric flashes referred to as 'Elves'. Geophys. Res. Lett., **24**, 583–586.

Ishaq, M. and Jones, D.L. (1977): Methods of obtaining radiowave propagation parameters for the Earth-ionosphere duct at ELF. Electron. Lett., **13**, 254.

Ishii, M., Fujii, F., Hidayat, S. and Sugita, A. (2002): Evaluation of JLDN based on observation during 2000–2002. Proc. 17th Int'l Lightning Detection Conference, Paper No. 39, Tucson, Arizona.

Jones, D.L. (1967): Schumann resonances and e.l.f. propagation for inhomogeneous, isotropic ionospheric profiles. J. Atmos. Terr. Phys., **29**, 1037–1044.

Johnson , M.P., Inan, U.S. and Lev-Tov, S.J. (1999): Scattering pattern of lightning-induced ionospheric disturbances associated with early/fast VLF events. Geophys. Res. Lett., **26**, 2363–2366.

Milikh, G.M., Papadopoulos, K. and Chang, C.L. (1995): On the physics of high altitude lightning. Geophys. Res. Lett., **22**, 85–88.

Nickolaenko, A.P. and Hayakawa, M. (1995): Heating of lower ionosphere electrons by lightning electromagnetic radiation. Geophys. Res. Lett., **22**, 3015–3018.

Nickolaenko, A.P. and Hayakawa, M. (2002): Reasonance in the Earth-Ionosphere Cavity. Dordrecht, Kluwer Acad. Pub., 288 p.

Pasko, V.P., Inan, U.S., Taranenko, Y. and Bell, T.F. (1995): Heating, ionization and upward discharges in the mesosphere due to intense quasi-electrostatic thunderscloud fields. Geophys. Res. Lett., **22**, 365–368.

Pasko, V.P., Inan, U.S., Bell, T.F. and Taranenko, Y.N. (1997): Sprites produced by quasi-electrostatic heating and ionization in the lower ionosphere. J. Geophys. Res., **102**, 4529–4561.

Reising, S.C., Inan, U.S., Bell, T.F. and Lyons, W.A. (1996): Evidence for continuing current in sprite-producing cloud-to-ground lightning. Gephys. Res. Lett., **23**, 3639–3642.

Rodger, C.J. (1999): Red sprites, upward lightning, and VLF perturbations. Rev. Geophys., **37**, 317–336.

Takeuti, T. and Nakano, M. (1983): Study on winter lightning activity in Hokuriku. Tenki, **30**, 13–18 (in Japanese).

Wait, J.R. (1996): Electromagnetic Waves in Stratified Media. Piscataway, IEEE Press, 372 p.